CS 285 Final Project: The Vertical Street

Toby Mitchell and Pardeep Kumar

December 16, 2011

1 Introduction

This paper describes the final course project in Professor Carlo Sequin's Digital Solid Modeling and Fabrication course at Berkeley. The idea for the project originated years ago in Toby Mitchell's idle investigations into shell structures during Fall 2007 winter break. The unbeatable material efficiency of shell structures, which behave like an arch in 3D, eventually inspired this work.

The pressure to house and sustain the world population has fostered haphazard expansion and sprawl. Especially in America, the surburban ideal has lead to an enormously wasteful use of resources. Large numbers of people claiming individual fiefdoms of lawn, garage, and yard have erased wild areas, polluted groundwater, and fostered a car-centric economy that requires a constant supply of fossil fuels. But in better-planned urban areas, where density is used to minimize environmental impact, the existing template is the high-rise tower, where inhabitants are sectioned into stacked boxes with little public space between them and minimal interaction with the street below. This standard pattern of high-rise development has been as extensively critiqued as the pattern of suburban sprawl, most famously by Jane Jacobs, but more significantly by the great numbers of people who still prefer the sprawl to the city.

We think that the most vital aspect of urban life is the street, and especially the streetside space between the roadway and the buildings. This is where the life of a city happens - in parks and squares and cafes and shops, where people meet their neighbors and their friends in a series of unplanned encounters that builds up the sense of connection that we need to feel part of a larger whole. Both the mandatory automobility of sprawl and the stacked boxes of the high-rise tower slice this artery of public life, eliminating the most essential space that cities require to feel like a place and not merely a location.

So how do we mesh streets and streetsides with the high-rise towers needed to make urban density possible? As structural engineers, the answer seems fairly clear: wind a street around a tower. Acheiving this new type of urban density, where public streets and their attendant sidewalks, parks, shops and apartments extend vertically into the towers of the city, is the main idea of this project.

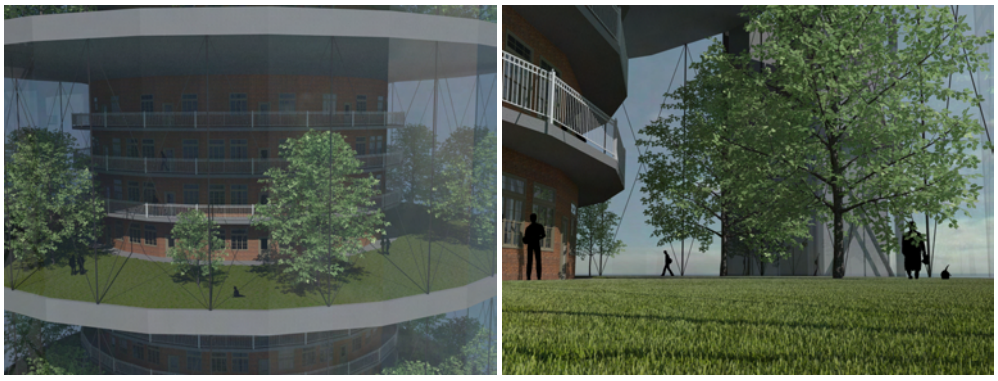

Figure 1: Extension of neighborhood space in the vertical direction. Apartments are stacked up tower with park space ringed around them.

2 Previous Work

In spring of 2008, Toby Mitchell along with Will Godfrey, Noel Vivar, and Lily Rong won a sustainable design competition sponsored by Autodesk with a design for a tower that prefigures the current work. In this tower, the conventional floor-by-floor format of the tower was used (as opposed to the continuous street), but with large local park spaces around the residences (Figure 1).

The tower was made physically possible by a structural system that acts like an arch bridge, enabling large column-free spans for the parks and apartments to fill. Like an arch bride, the system is composed of a flat deck supported by vertical members by an arched surface that channels the loads on the deck down to the supports. Unlike an arch bridge, there is only one support at the center column, so the horizontal thrust required at the outer edge of the arched surface must be provided by a series of tensioned cables stretching straight at deck level between the outer edge and the large concrete central core support. These half-arch sections are then revolved around the center column to create a series of floors (Figure 2).

The material efficiency of this structure, which, like an arch bridges, channels loads in the plane of the structure and therefore largely avoids the out-of-plane bending that would lead to impossibly oversized members, allows it to be constructed at large scales. At the time, we anticipated that this type of structure could effectively stack city blocks vertically, getting closer to the ideal of the public-private intersection of the street (Figure 3).

Will Godfrey, who also did the renders presented here, remarked that it would be even more interesting to do the same sort of structure along a continuous spiral path. At the time, Mitchell lacked the mathematical ability to describe the spiral version of this structure. But the idea stuck, and was picked up again years later for this class project.

Figure 2: Structure consists of floors where the concrete floor deck is supported on a curved concrete shell. The shell is revolved around a center column, with services in external structures at the outer rim.

3 Derivation of the Spiral Shell Surface

The key ingredient to making the vertical street work in practice is the selection of the right shape for the curved support shell that channels the weight of the buildings and other features of the street down into the central supporting core. The correct shape can be derived by looking at the equations of equilibrium of a shell surface in polar coordinates:

r-direction force balance, for forces projected to the r-θ plane: where

$\frac{\partial}{\partial r}(r\bar{N}_r) + \frac{\partial \bar{N}_{\theta r}}{\partial \theta} - \bar{N}_\theta = 0$

θ-direction projected force balance:

$\frac{\partial \bar{N}_\theta}{\partial \theta} + r\frac{\partial \bar{N}_{r\theta}}{\partial r} + 2\bar{N}_{r\theta} = 0$

z-direction projected force balance:

$\left[\frac{1}{r^2}\frac{\partial^2 z}{\partial \theta^2} + \frac{1}{r}\frac{\partial z}{\partial r}\right]\bar{N}_\theta + 2\left[\frac{1}{r}\frac{\partial^2 z}{\partial r \partial \theta} - \frac{1}{r^2}\frac{\partial z}{\partial \theta}\right]\bar{N}_{r\theta} + \frac{\partial^2 z}{\partial r^2}\bar{N}_r = w$

where forces in a (non-orthogonal) frame in the tangent space of the shell are given by

r-projection:

$\bar{N}_r = \hat{N}_r \frac{\sqrt{1+z_{,\theta}^2/r^2}}{\sqrt{1+z_{,r}^2}}$

θ-projection:

$\bar{N}_\theta = \hat{N}_\theta \frac{\sqrt{1+z_{,r}^2}}{\sqrt{1+z_{,\theta}^2/r^2}}$

shear projection:

$\bar{N}_{r\theta} = \hat{N}_{r\theta}$.

, subscripts denote differentiation with respect to the subscript variable following the comma.

Similar equations in Cartesian coordinates are discussed in Timoshenko's classic "The Theory of Plates and Shells".

In the classical examples, one is given a shell shape and solves for the stresses

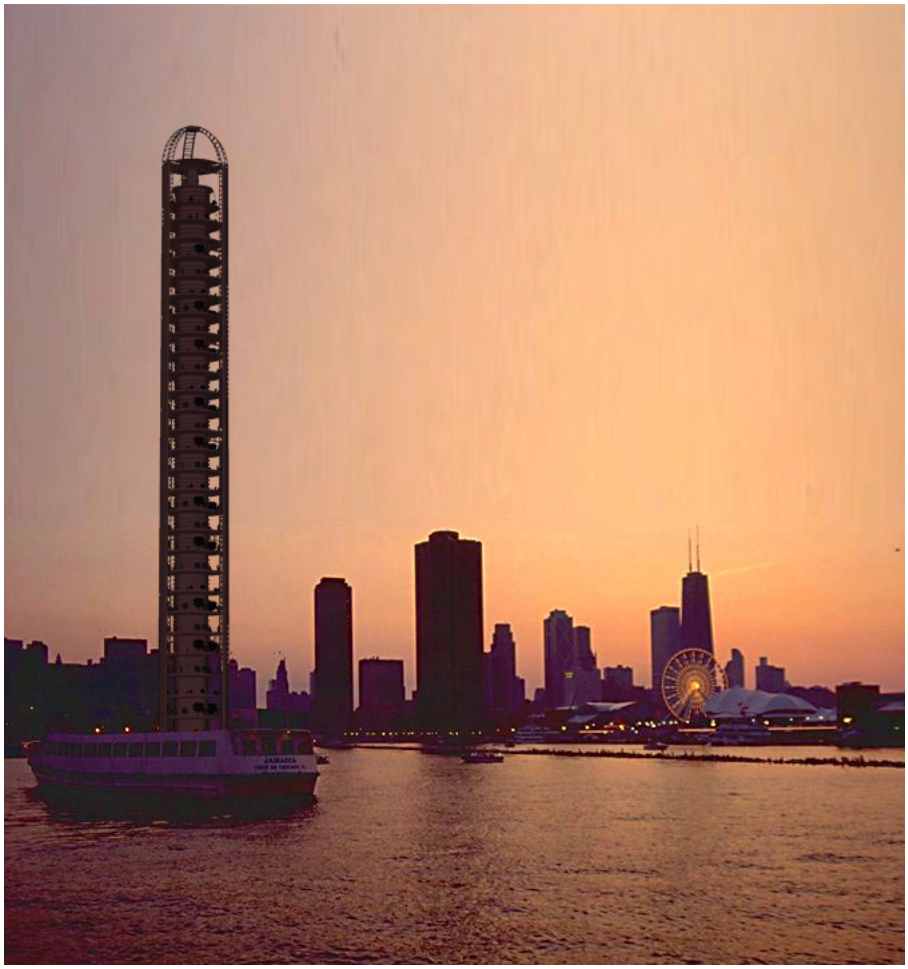

Figure 3: The limit on the scale of the structure is determined mostly by economics, not physics. Quite large projects could be constructed that open up large vertical neighborhood spaces.

in the shell. However, in "Equilibrium of Shell Structures", Heymann points out that, in the absence of bending, one can also assume a desired stress distribution *first*, and then solve "backwards" to determine the shape of the shell. That is, in the case of pure in-plane (membrane) loads, the shell is statically determinate. This is the approach we take.

3.1 Derivation of Profile Curve

Assume a radially symmetric profile curve

$z = f(r)$ with inner edge at radius r_i and outer edge at radius r_o.

under constant uniform loading w.

This corresponds to a circular slab supported by a shell whose weight is negligible in comparison to the applied loads, as we'd roughly expect to see for the loads from a street.

In this case, it is reasonable to *assume* $\bar{N_\theta} = \bar{N_{r\theta}} = 0$ will give a solution.

We impose symmetry conditions:

$\frac{\partial \bar{N_\theta}}{\partial \theta} = \frac{\partial \bar{N_{r\theta}}}{\partial \theta} = \frac{\partial \bar{N_r}}{\partial r} = 0 \Rightarrow \theta$-balance is trivially satisfied.

The r-direction balance then becomes:

$\frac{\partial}{\partial r}(r\bar{N_r}) = 0 \Rightarrow \bar{N_r} = -\frac{A}{r}$, where A is a constant (assumed positive). The - sign follows from the fact that forces in the shell must be compressive if we wish to find a solution that can be supported by a column. Note that the above implies that a reaction force A/r_o must be provided at the outer edge and a corresponding force A/r_i at the inner edge. This can be done either by a cable encircling the outer edge or a series of radial tie-backs anchoring the outer edge to the inner column.

The shape of the profile curve $z = f(r)$ can be deduced from the z-balance equation:

$\frac{\partial^2 z}{\partial r^2}\bar{N_r} = w$, $\bar{N_r} = -\frac{A}{r} \Rightarrow \frac{\partial^2 f}{\partial r^2} = -\frac{wr}{A} \Rightarrow$

$\frac{\partial f}{\partial r} = -\frac{wr^2}{2A} + B \Rightarrow$

$f(r) = -\frac{wr^3}{6A} + Br + C.$

Thus the profile of the support shell that will bear the applied loads in in-plane compression (i.e., a membrane state of stress) is a cubic curve. It remains for us to determine the constants that specify this curve.

3.2 Boundary Conditions

Since a concrete slab is assumed to sit atop the shell and attach to the shell at r_o, it is natural to set the zero-level of $f(r)$ at r_o. This allows us to eliminate the constant C:

$f(r_o) = 0 \Rightarrow C = \frac{wr_o^3}{6A} - Br_o \Rightarrow$

$f(r) = -\frac{w}{6A}(r^3 - r_o^3) + B(r - r_o).$

Since we'd like to provide the needed outer edge reaction with a circular cable or set of radial tie-backs, we need the edge of the profile curve to lie flat on the r-θ plane so that the cable is in line with the floor slab. This will eliminate the constant B:

$\frac{\partial f}{\partial r}(r_o) = 0 \Rightarrow B = \frac{wr_o^2}{2A} \Rightarrow$
$f(r) = \frac{w}{6A}\left[(r_o^3 - r^3) + 3r_o^2(r - r_o)\right]$.

Finally, we'd like to be able to set the total depth d of the profile curve between the inner and outer radii. Since $f(r_o) = 0$, we have
$f(r_i) = -d \Rightarrow A = -\frac{w}{6d}\left[(r_o^3 - r_i^3) + 3r_o^2(r_i - r_o)\right] = \frac{w}{6d}\left[(r_i^3 - r_o^3) + 3r_o^2(r_o - r_i)\right]$.
Note that in order for A to be positive as defined, we must have
$3r_o^2(r_o - r_i) \geq r_o^3 - r_i^3$
which indicates that we must have $r_o \geq r_i$.

Thus the shape of the profile curve in terms of inner radius r_i, outer radius r_o, and profile depth d is
$f(r) = d\left[\frac{(r_o^3 - r^3) + 3r_o^2(r - r_o)}{(r_i^3 - r_o^3) + 3r_o^2(r_o - r_i)}\right]$,
and the horizontal force in the supporting shell is
$\bar{N_r} = -\frac{A}{r} = -\frac{w}{6dr}\left[(r_i^3 - r_o^3) + 3r_o^2(r_o - r_i)\right]$.
Writing
$\frac{\partial f}{\partial r} = \frac{3d(r_o^2 - r^2)}{(r_i^3 - r_o^3) + 3r_o^2(r_o - r_i)}$,
recalling the definition of the r-projection, and noting the fact that $z_{,\theta} = 0$ in the current case gives
$\hat{N_r} = -\frac{A}{r}\sqrt{1 + f_{,r}^2} = -\frac{w}{6d}\sqrt{\frac{\left[(r_i^3 - r_o^3) + 3r_o^2(r_o - r_i)\right]^2}{r^2} + 9\frac{d^2}{r^2}(r_o^2 - r^2)^2}$,
and since this is already in an orthogonal frame (since the fan floor shell is a surface of revolution) we can write $N_r = \hat{N_r}$. Note that $N_r \to \infty$ as $r \to 0$, so we must keep $r_i > 0$ for the solution to have physical meaning.

We note that though this profile curve was derived for a flat slab, the curve is exactly the same for a helicoidal (spiral) slab. Proof of this fact is outside the scope of this report.

We also note that the real load conditions present on a tower, e.g., wind, will require additional consideration and will lead to additional reinforcement of the structural members in order to resist the bending forces inevitably introduced by these loads. However, it makes sense to start the design from the above gravity-loaded case, which the structure must always resist. One then has money in the bank, structurally speaking, that can then be invested in resisting the loads from wind, earthquake and other less predictable forces.

4 Design Decisions

The focus of CS 285 was the fabrication of parts using 3D printing and other digital fabrication techniques. Since the shape of the support structure is key to its performance, it makes a great deal of sense to control this geometry as precisely as possible by 3D-printing the *joints* of the structure, since they effectively control its geometry. This lead to our project proposal: build a scale model of the vertical street by 3D-printing the joints of the structure, and then mapping a grid of straight lines onto the structure that frame between these joints and approximate the ideal continuous shape of the shell.

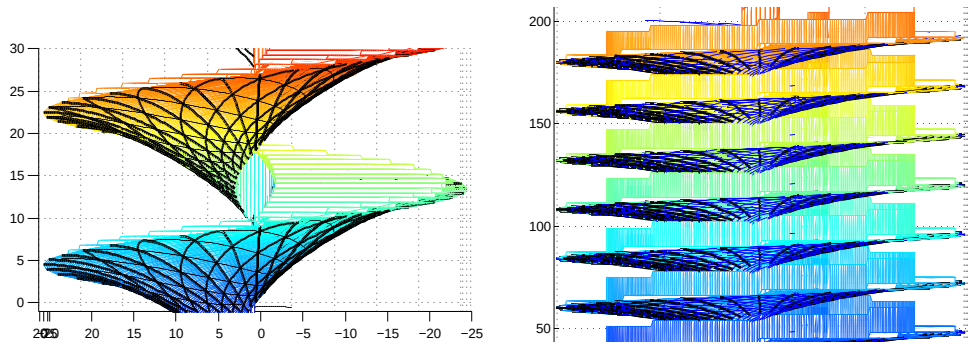

Figure 4: Spiral stair with cross-bracing. The structural principle could be extended to full-sized buildings, leading to a tower with a street winding its height.

Physically, diagonal cross-bracing was required to allow the structure to resist any twisting (torsional) loads that might be applied to it, for example by wind forces. The cross-bracing pattern was arrived at by tracing two counter-rotating logarithmic spirals onto the surface of the shell. Since this pattern of braces is the ideal form for resisting torsional loads in the 2D plane (as discovered by Michell in "The Limits of Economy of Material in Frame-Structures"), it should provide the most efficient scheme for resisting torsion in the plane of the shell. The exact continuum shell shape and the spiral bracing were generated in MATLAB (Figure 4).

The points of intersection of these cross-bracing spirals also determine the grid of points on the surface of the shell that we interpolate with straight lines to get a structure we can easily construct from steel rods. With this scheme, one has to choose the number of spirals, as well as the number of radial ribs that are the main load-bearing members. This was done by a process of trial and error, where the amount of points needed to accurately and aesthetically map the surface (the more points, the better) was balanced against the practical need for a building model that could be constructed in a reasonable time frame by two people (the fewer parts, the better).

In order to best approximate the Michell spiral structure of the cross-bracing, where the spirals cross at right angles, we adjusted the interpolation points so that the straight cross-bracing elements cross each other at right angles. The final design balanced the concerns of accuracy and constructability as best as possible within the constraints of the project (Figure 5).

One detail that was somewhat subtle was that the choice of interpolation point locations could strongly affect the quality of the interpolated shape. For instance, we noticed that, for the five-ringed design we settled on, extending fully cross-braced squares to the outer edge led to a radial rib geometry that was noticeably kinked near the edge (Figure 6). This happened because the shell profile is nearly straight at the center column (the linear term of the profile

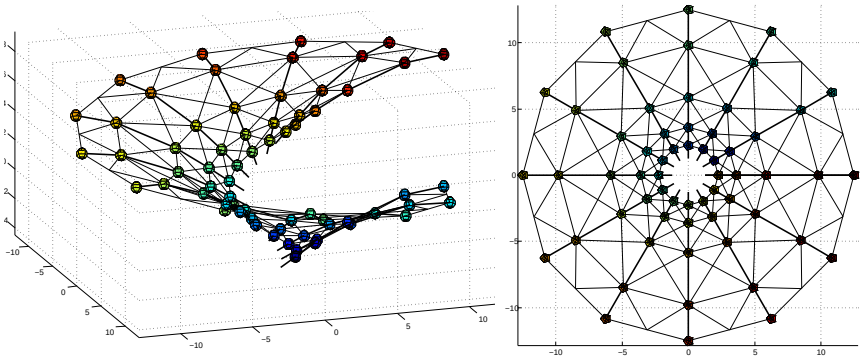

Figure 5: The final design is created by linearly interpolating the continuous shell surface at a set of points. The points were chosen so that the diagonal braces cross at right angles.

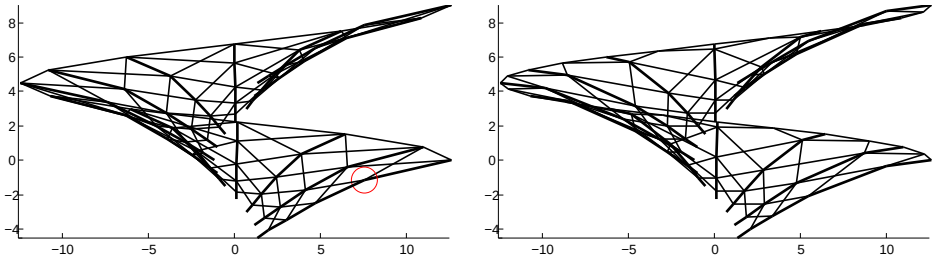

Figure 6: Original interpolation led to a sharp kink (red circle). Interpolating with a half-length made the rib curve more smoothly.

equation dominates), becoming progressively more curved at the outer edge. Since the cross-braced squares become larger near the outer edge, one has fewer points to map a more strongly curved surface, leading to a noticeable inaccuracy.

By contrast, using a half-square at the outer edge looked somewhat less symmetric overall, but lead to a more gracefully curved rib shape. We decided to use this as our final design.

Design-wise, the most labor-intensive part of the model was the design of the joints that were to be 3D-printed. Starting with the MATLAB model of the interpolated structure, the locations of the joints were exported as a .stp file from MATLAB into Rhino, connected with solid pipes, surrounded by solid spheres, and then the pipes were Boolean-subtracted from the spheres to generate sockets in the spheres into which the steel rods could fit. Care was taken to ensure that rods did not physically interfere with one another. In order to keep the cost of the joints down, the spheres were carved away through further Boolean operations into complicated socketed objects that just surrounded the inserted rods.

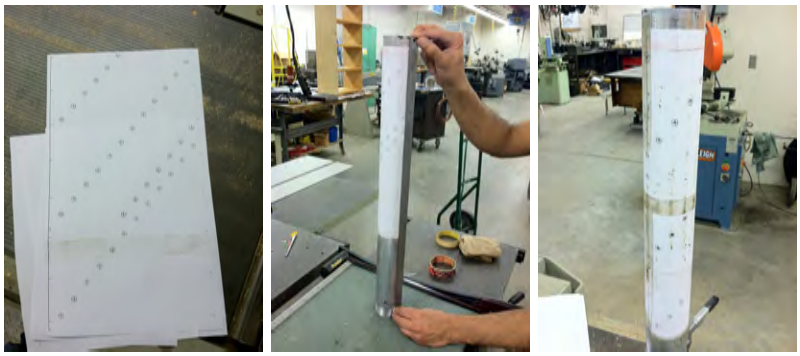

Figure 7: Drill hole locations were printed directly from MATLAB onto a sheet of paper. Paper was then wrapped around the center column pipe. This resulted in well-aligned drill holes for the tie-back inlets and outlets.

Care was also taken to ensure that the CAD files for each joint were perfectly seamless and non-self-intersecting, since this is necessary to ensure that the 3D-printing of the joints is accurate. Once done, the joints were exported to .stl files, and the .stl files were checked over for consistency and then sent to Shapeways.com for fabrication out of laser-sintered nylon powder. There was a two-week lead time for this process, so very early on we printed some simple test joints to ensure that our rods would fit correctly before we placed our main order.

5 Building the Model

While waiting for the joints to arrive from Shapeways, we fabricated all the other parts of the model.

A 24 in steel pipe section with outer-diameter of 2.5 in and thickness of 0.25 in was used as the central shaft. The central shaft supported the helical rings and cable tie backs. Depending on the orientations two sets of holes were drilled in the central shaft: horizontal holes for cable tie backs and inclined holes to support the rib rids of the inner most helical ring.

Location of holes on the central shaft was an important step, as wrong locations could lead to inaccurate geometry and an unstable model. The holes locations were carefully measured from the MATLAB model and printed on a sheet of paper, scaled appropriately to fit the actual dimensions of the model. This sheet was wrapped around the circumference of the central shaft and taped tightly (Figure 7).

The steel pipe section was clamped tightly to a horizontal platform of the drill machine, and locations of holes were tapped using a tap bit. After than maintaining the same position, horizontal holes for cable tie back were drilled. The platform was then tilted to orient it at an angle of 32 degrees with respect to the vertical. The clamp was positioned and its angle was checked again.

Figure 8: Drill press was set up at an angle of 32 degrees to drill and tap holes. Fit was tested with 1/4" bolts. Alignment of bolts was accurate. Bolts were then cut to length to produce the innermost ring of rib rods.

Figure 9: Rods were cut, leaving metal flash. This was ground down, and the ends were beveled. Final rod length was checked with digital calipers. Rods deviated upwards a maximum of 20 mils from the target length, and downward a minimum of -5 mils.

The central shaft was then clamped with two flat wooden blocks on either side (Figure 7). The flat wooden blocks assured proper clamping and resisted the rotation of the central shaft about axis perpendicular to its circular section. Inclined holes for the rib rods were then drilled at the tapped locations.

The helical part of the model comprised of following:

1. Rib Rods: Rib rods connect the helical rings. They were oriented in the radial direction. All rib rods were 0.25 in diameter. The rib rods connecting the innermost helical ring with the central shaft were threaded. The rest of the rib rods had plain surface.

2. Helix Rods: Helix rods were oriented along the circumference of the helical rings. Plain rods with 0.1875 in. diameter were used as Helix rods.

3. Cross Braces: Bracing system of the model comprised of cross braces. Plain steel rods of diameter 0.125 in were used for making the cross bracing system of the structure.

4. Vertical Tie Rods: 0.125 in threaded rods were used for the vertical tie

Figure 10: Joints contained leftover nylon powder that had to be removed with a paperclip. The assortment of finished parts was laid out prior to assembly.

system. The main function of these rods was to support the cable ties and the horizontal deck.

All the rods explained above were cut out to required length using bar cutting lathe machine (Figure 9). These rods were than sanded to chip of the sharp edges on a sand machine. The lengths were adjusted to be within an error of + 20 and -5 mils, based on the measurements made using a digital caliper.

5. Joints: Based on their locations joints were labeled as primary and secondary. Primary joints were ones connecting the rib rods, helix rods, cross braces and vertical tie rods. They were distributed all long the helical assembly. Secondary joints connected helical rods and cross braces. They were positioned only at the outer most helical ring. Inside surfaces of all the joints were cleaned to remove residual material from construction of the joints (Figure 10).

6. Cable Ties: To get the proper force transfer due to the self weight or imposed weight on the deck, cable ties were run through each rib arch. Brake cables of diameter 0.01325 in were used as cable ties. These cables were screwed with each vertical tie rod, passed through one face of the central shaft and tied back at the other diametrically opposite end. A hollow screw was used to let the cable loop pass and clamp the ends firmly. However, our biggest mistake was that we ordered slightly less than the necessary amount of cable since we didn't account for the slack needed to adjust the cable length properly. Pending further cable, these are left out of the final assembly.

7. Plexi-glass Decks: Plexi-glass decks were supported by the vertical tie rods from two adjacent rib rods on each side. The shapes were cut as shown and the holes were carefully drilled at required locations. These decks were held in place using nuts.

After all the parts were ready the central shaft was cleaned and properly placed in the wooden foundation blocks. The innermost helical ring was installed first. After that the assembly was hammered lightly using a rubber mallet to ensure a rigid connection between the joints and the connecting rods (Figure 11). After that rest of the structure was assembled one ring at a time (Rib

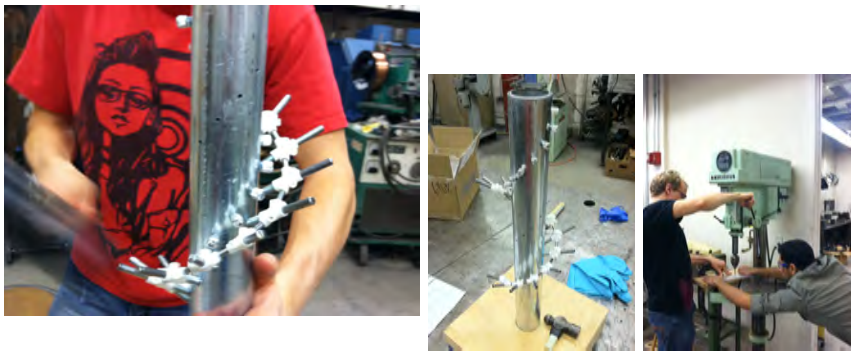

Figure 11: Joints were hammered to a tight fit. Each ring of joints was assembled as a unit. The final fabrication step was the cutting and drilling of the plexiglass steps of the staircase.

rods, helix rods and cross braces) followed by light hammering to ensure firm connection. Once the arch assembly was ready the vertical threaded tie rods were screwed into the joints. After that the plexi-glass deck was screwed using nuts and positioned horizontal on the vertical threaded rods of adjacent ribs.

The final result hewed very closely (as expected!) to the CAD model of the design. Though coarse, it acheived some hint of the elegance and strength that shell structures can embody (Figure 12).

6 Conclusions and Future Work

The final model proved that the complex geometry of shell structures can be accurately constructed through careful design of component parts and 3D digital fabrication of joints. This approach is particularly useful because it allows all the parts besides the joints, e.g., the structural members themselves, to be fabricated with conventional machine shop techniques, meaning that the relatively expensive 3D fabrication of parts can be limited to the joints where the added accuracy of 3D fabrication is most needed.

In order to test the structure under the design loads (uniform gravity loading of the plexiglass steps), we need to order a new run of cable and reframe the structure with the cable in place and tightened to the appropriate tension. Even prior to doing this, however, it is clear from working with the model during assembly that the small eccentricities (that is, failures of the connecting rods or cable ties to line up directly with the center point of the joints) that were designed in to the model to facilitate construction of the tie-backs and to avoid clashes between the rods inside the joints may have a significant effect on structural behavior.

In particular, the tie-back was designed somewhat off-center from the edge joint in order to facilitate easy joining of the cable to the joint. However, this will introduce some bending into the joint, limiting the performance of the structure.

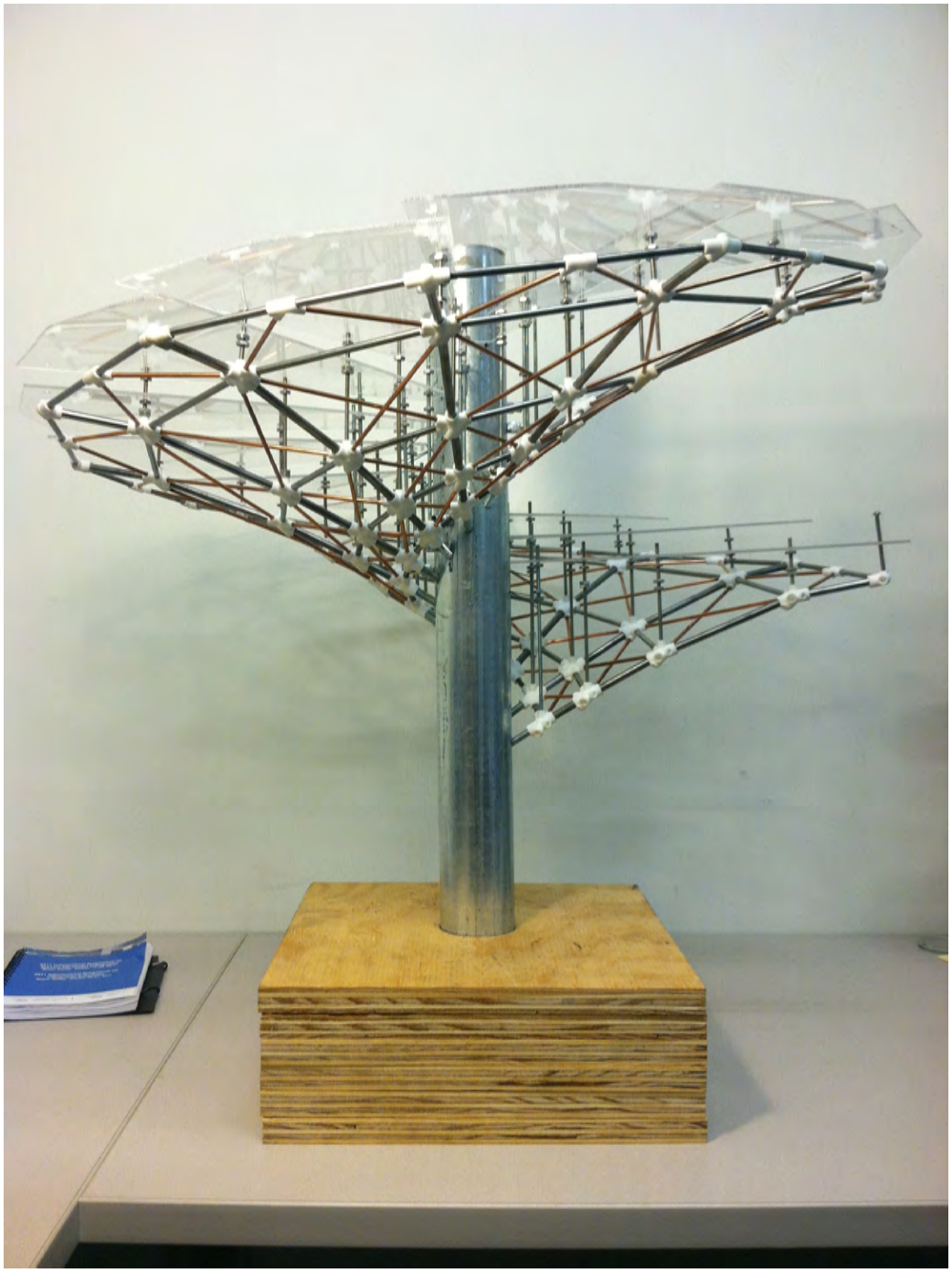

Figure 12: The final product.

It is worth noting that these issues would not be present if the structure were built at larger scales, since the design of the joints was limited by the ability of the authors to manipulate them manually. At larger scales, this is easily avoided by careful joint design.

Ideally, this report will be updated soon with measurements of the displacement of the structure under load, once the cable tie-backs are completed.

7 Acknowledgements

This project would have been impossible without the financial support for the purchase of materials contributed by Professors Carlo Sequin and Sanjay Govindjee. The Civil Engineering Department lab staff - Jeff Higginbotham and Matt Cataleta - provided generous assistance in the form of their time and expertise in the Davis Hall machine shop. We are extremely grateful for their support and assistance.